

# Modeling of the Heat Transfer Between a CO<sub>2</sub> Sequestration Well and the Surrounding Geological Formation

Benjamin Sponagle<sup>1\*</sup>, Mumuni Amadu<sup>2</sup>, Dominic Groulx<sup>1</sup> and Michael J. Pegg<sup>2</sup>

<sup>1</sup>Mechanical Engineering Department, Dalhousie University

<sup>2</sup>Process Engineering and Applied Science Department, Dalhousie University

\* Corresponding author: P.O.Box 15 000, Halifax, Nova Scotia, Canada, B3H 4R2, bn458906@dal.ca

**Abstract:** A 1 km deep carbon sequestration well was simulated using COMSOL Multiphysics 4.2. Utilizing the heat transfer and fluid flow modules, a flow of super critical carbon dioxide was modeled as it was injected down a well. The goal was to determine the temperature gradient in the earth around the assembly due to the injection. A model of the system with laminar injection rates was successfully created. Simulations with velocities of 0.001 and 0.01 m/s showed that there was heat transfer from the fluid to the formation surrounding it near the injection inlet. However, further down the well from the injection site the heat transfer changed direction, the formation transferring heat to the fluid at that point. The depth of this inversion point was approximately 117 and 619 m respectively for those two velocities. The current simulations indicate that as the injection velocity was increased the depth of the inversion point increased. Future simulations will centre on simulating higher velocity turbulent flows, using the CFD module, which are more representative of the injection rates which would be seen in an actual carbon sequestration project.

**Keywords:** Supercritical CO<sub>2</sub>, Laminar Thermal Flow, Carbon Sequestration, Semi-infinite Medium.

## 1. Introduction

The effects of climate change and the release of greenhouse gasses are a continuing concern for governments and industry. Current renewable technologies are not capable of replacing fossil fuels as the world's primary source of energy. Therefore, technologies that allow for the capture and sequestration of carbon emissions from conventional energy generation facilities remain a field of interest.

One possible method for the mitigation of CO<sub>2</sub> emissions is sequestration in depleted oil reservoirs. CO<sub>2</sub> would be pumped down a well and into the reservoir at supercritical temperatures and pressures where it would remain trapped and be prevented from reaching the atmosphere.

An important consideration with this type of technology is the long term stability of the reserve. One factor that may be important in the stability of

such reservoirs is the extent to which the cap rock is damaged during the injection process.

The goal of these simulations is to thermally model the injection well and investigate the temperature gradient developed in the cap rock as well as determine in the inversion depth in the temperature and the heat flux of the supercritical CO<sub>2</sub>. Ultimately, results from this study will lead to an assessment of the thermal stress on the cap rock during injection [1-4].

## 2. Geometry and Materials

A well assembly for this type of injection setup generally consists of six different domains: injection fluid, tubing, annulus (consisting of thermal insulation, Aerogel), the outer casing, the cement layer surrounding the well and the geological formation (See Fig. 1). The dimensions used for each of the domains are shown in Table 1. The well was modeled to be 1 km deep and 50 m of ground around the well assembly was simulated in order to account for the semi-infinite nature of the surrounding ground.

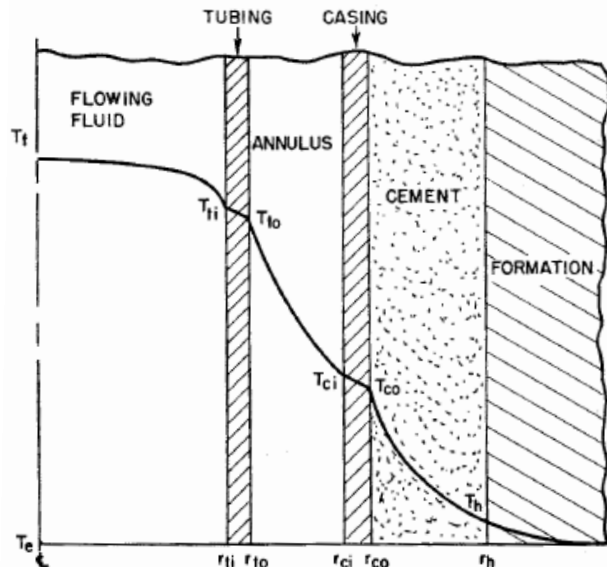


**Figure 1.** Geometry used for the carbon sequestration well modeled [4].

**Table 1.** Dimensions and materials used in each of the simulated domains.

Domain	Dimensions	Material
<b>Tubing inner radius</b>	1.221 in (3.101cm)	CO <sub>2</sub>
<b>Tubing</b>	0.215 in (0.546cm)	Steel (ASIS 4340)
<b>Annulus</b>	1.700 in (4.318cm)	Aerogel
<b>Casing</b>	0.362 in (0.919cm)	Steel (ASIS 4340)
<b>Cement</b>	1.313 in (3.335cm)	Portland Cement
<b>Formation</b>	50 m	Shale and Brine

**Table 2.** Thermophysical properties of the materials modeled

Material	Density (kg/m <sup>3</sup> )	Thermal Conductivity (W/(mK))	Specific Heat (J/(kgK))
<b>ASIS 4340 Steel</b>	7850	44.5	475
<b>Aerogel</b>	140	0.024	0.84
<b>Portland Cement</b>	3100	0.3	750
<b>Formation</b>	2300	1126.56	1.42

**Table 3.** Element counts in the various domains

Formation Component	Horizontal Element Count	Vertical Element Count
<b>Fluid Flow</b>	20	5000
<b>Pipe Wall</b>	5	5000
<b>Annulus</b>	5	5000
<b>Casing</b>	5	5000
<b>Cement</b>	5	5000
<b>Formation</b>	5	5000

The injection fluid was modeled as pure supercritical CO<sub>2</sub>. The material properties of supercritical fluids are strongly temperature dependant. Those properties were incorporated in COMSOL as tables and modelled using interpolation functions based on data from the NIST Standard Reference Database 69 [5].

Tables 2 present the thermophysical properties of: steel, aerogel, portland cement and the formation. The formation was modelled as being one continuous solid material. The material properties were calculated as the mass volume average of the solid and fluid components (shale and brine respectively). This is a simplification and the simulation could be

expanded to include stratification and/or porosity when modeling the formation.

### 3. Use of COMSOL Multiphysics

COMSOL Multiphysics 4.2 was used to model the heat transfer between the injection assembly and the surrounding geology. The model is axisymmetric. The heat transfer and CFD modules were used in the simulation. The system was meshed using a mapped mesh. A much higher resolution is required within the fluid flow domain than in the solid heat diffusion domains; especially far from the injection assembly where it very little changes are recorded because of the semi-infinite nature of the problem. The distribution of the nodes in the fluid flow domain was arranged so that there is a higher concentration of nodes in the boundary layer region of the flow (see Figure 2). Table 3 summarizes the distribution of nodes in each of the domains within the model.

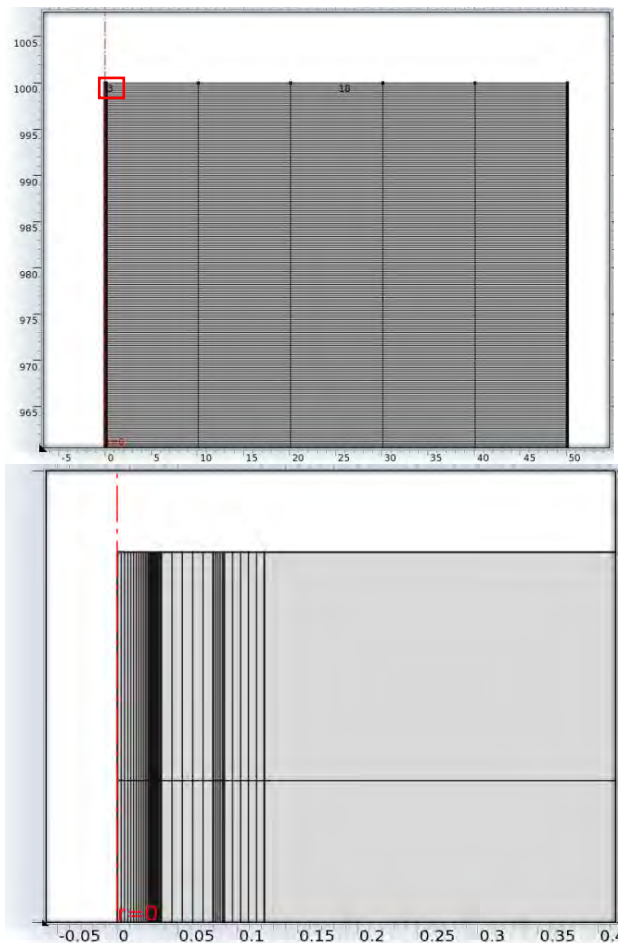


**Figure 2.** Mapped mesh used in the simulation.

The CO<sub>2</sub> is injected at 318K and a pressure of 100 bar. The top boundary condition is set at 283K in order to reflect the temperature of the ground at the point which it remains constant and is not affected by surface fluctuations. The natural temperature gradient (~25 K/1000 m) that exists in the earth's crust is set as an initial condition and is modelled using a constant heat flux at the bottom boundary. This heat flux is calculated using Eq. (1) and has a value of 0.0355 W/m<sup>2</sup>.

$$Q = k_f \times \left(\frac{dT}{dz}\right) \quad (1)$$

$$1.42 \text{ W/(mK)} \times \left(\frac{25\text{K}}{1000\text{m}}\right) = 0.0355 \text{ W/m}^2 \quad (2)$$

The outer edge of the simulated domain is held at the natural temperature gradient to produce a semi-infinite system. From Fig. 5, it can be seen that the temperatures do not vary anymore 50 m from the injection assembly, demonstrating that the system does behave as a semi-infinite domain.

An injection rate that would be representative of an actual carbon sequestration project is 26 kg/s. This mass flow rate results in a Reynolds number of ~10<sup>7</sup> (variable with local material properties within the system). This is a highly turbulent flow. However, the current model uses smaller velocities which fall into the laminar flow regime.[1-4]

#### 4. Theory

The model is solving three different equations. The fluid domain models both the energy equation with diffusion and convective terms as well as the fluid flow equation. These equations are fully coupled by temperature and pressure dependant material properties. The full energy equation for the fluid flow domain is shown below.

$$\rho C_p \frac{DT}{Dt} = \nabla \cdot (k\nabla T) \quad (3)$$

where  $\rho$  is the density,  $C_p$  is the specific heat,  $k$  is the thermal conductivity. Note that the convective term is included in the material DT/Dt.

Heat transfer through the well assembly and formation were modeled using the simple conduction equation for heat transfer in a homogenous solid.

$$\rho C_p \frac{dT}{dt} = \nabla \cdot (k\nabla T) \quad (4)$$

The fluid flow was handled in two different ways. Several simulations were done at injection rates which were laminar. In this case the full compressible Navier Stokes equation was used.

#### 5. Results

The results from simulations to date have been done with injection rates within the laminar regime. These flow rates are significantly slower than those of the physical system but provide promising and interesting results.

The steady solution of a fully laminar flow with an injection velocity of 0.001 m/s is shown in Figs. 3 and 4. The arrows on Fig. 3 indicated the locations of the enlarged sections shown in Fig. 4.

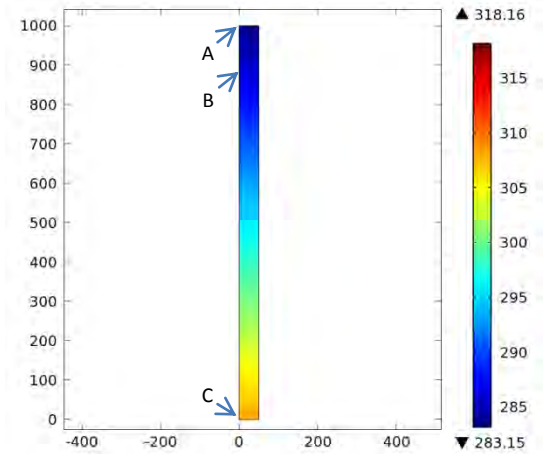


Figure 3. Surface plot of the temperature in the entire simulated domain.

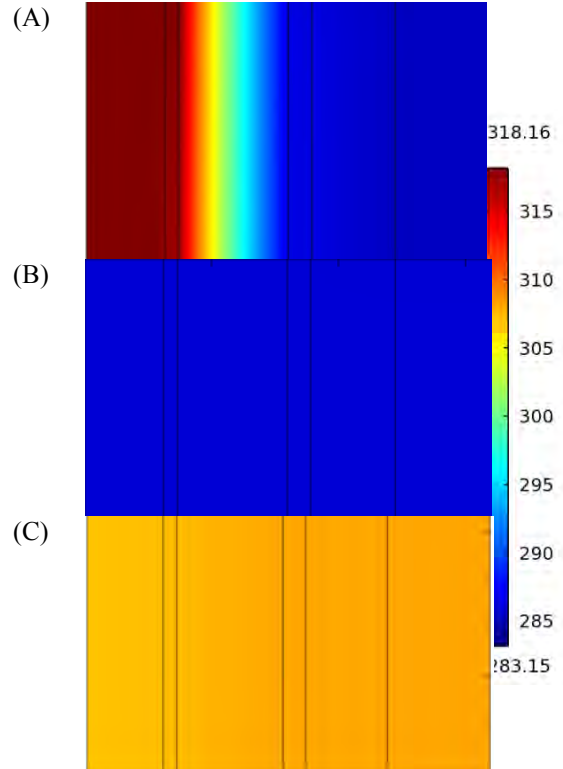
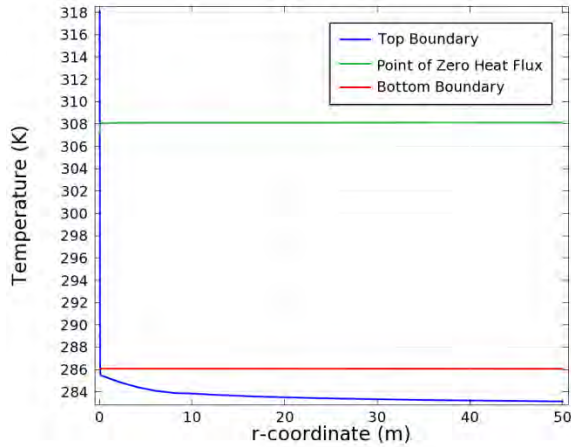


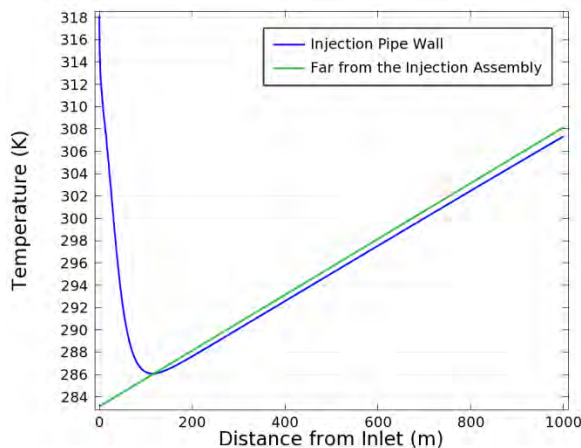
Figure 4. Three 0.1 m high, 0.15 m wide, Temperature distribution sections showing the inlet (A), position of zero heat flux (B) and outlet (C) of the injection assembly.

Figure 5 shows the temperature profile along the width of the system at the top and bottom boundaries as well as the point at which there is no heat flux to or from the fluid flow (0, 1000, and 117m from the inlet respectively). As expected, the region of the domain far from the injection assembly sees very little change in temperature in the  $r$  direction approximating an infinite system.



**Figure 5.** The temperature profile along the width of the system at different heights (inlet velocity = 0.001m/s).

If we plot the temperature profile at the wall of the injection pipe we can see that initially the fluid is transferring heat to the formation. However, at approximately 117m deep the temperature of the fluid reaches the temperature of the formation (see Fig. 6 and Fig. 7). As you go deeper the temperature of the formation increases and we see heat transfer from the formation to the fluid flow.



**Figure 6.** The temperature profile along the inner wall of the injection tubing and the temperature profile far from the injection assembly (inlet velocity = 0.001m/s)

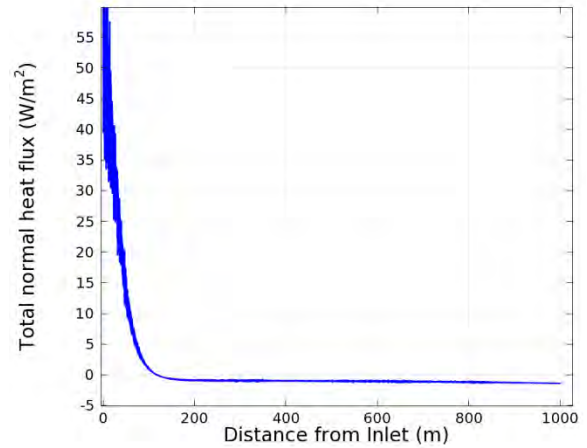


**Figure 7.** The heat flux at the inner wall of the injection tubing (inlet velocity = 0.001m/s)

The temperature of the fluid ranges from the injection temperature of 318K to a minimum of 286K. This results in large variation in the properties of the carbon dioxide along the length of the injection assembly. Figures 8 through 11 show the variation in these properties. The change in fluid density has a large effect on the velocity of the flow. Figure 12 shows the velocity at the centre point of the injection tubing plotted against the tubing's length. The velocity of the flow is reduced due to the large increase in density over the length of the injection tubing.

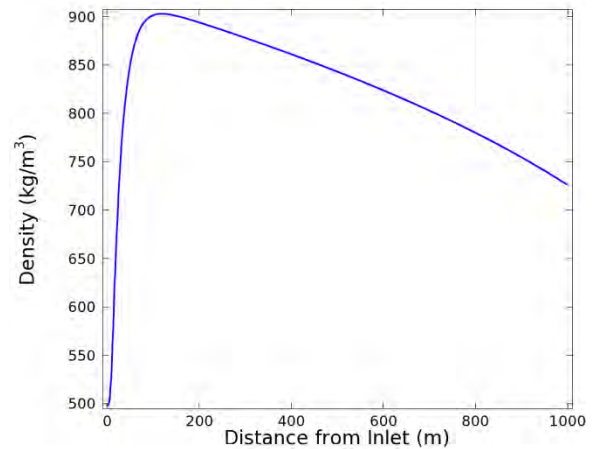


**Figure 8.** Density of the CO<sub>2</sub> at the centre of the injection tubing plotted against the tubing's length (inlet velocity = 0.001 m/s).

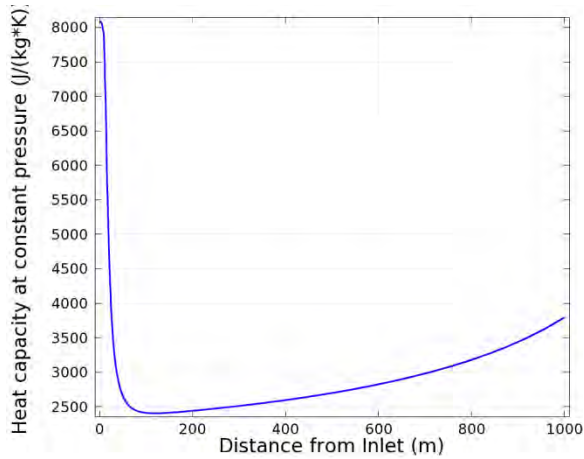


**Figure 9.** Specific Heat of the CO<sub>2</sub> at the centre of the injection tubing plotted against the tubing's length (inlet velocity = 0.001 m/s)

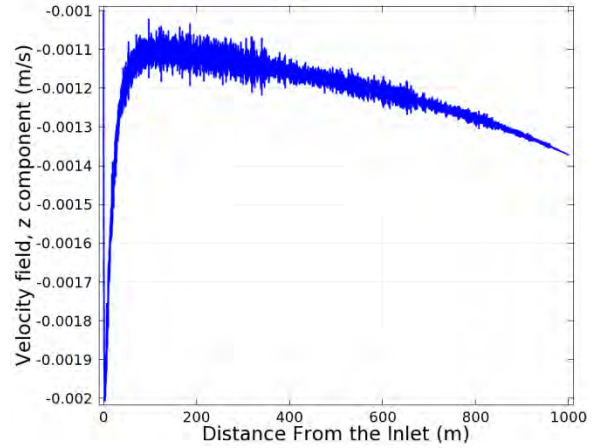


**Figure 12.** Velocity at the centre of the injection tubing plotted against the tubings length (inlet velocity = 0.001 m/s)

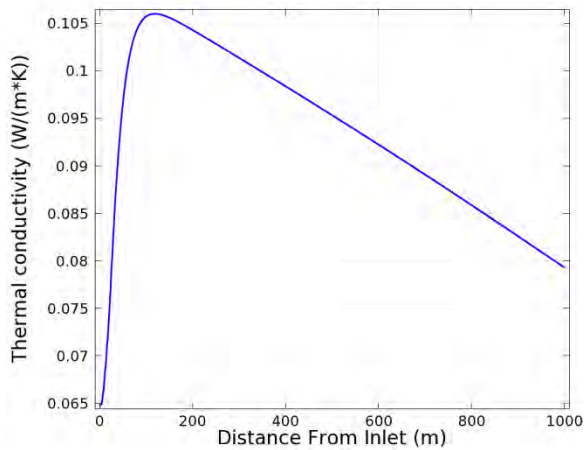


**Figure 10.** Thermal Conductivity of the CO<sub>2</sub> at the centre of the injection tubing plotted against the tubing's length (inlet velocity = 0.001 m/s)

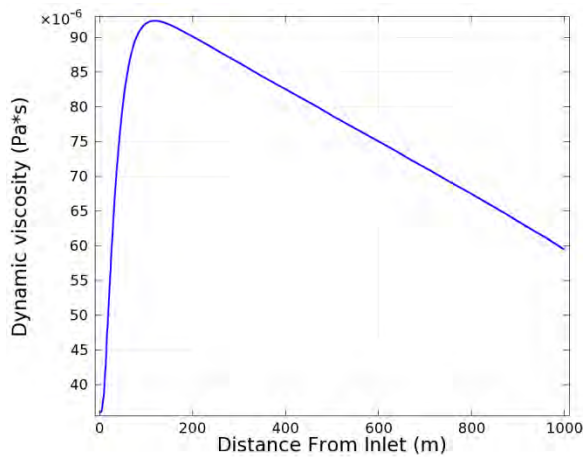


**Figure 11.** Viscosity of the CO<sub>2</sub> at the centre of the injection tubing plotted against the tubing's length (inlet velocity = 0.001 m/s)

If we increase the injection velocity to 0.01 m/s we can see the point at which the heat transfer shifts direction has moved deeper to approximately 619 m (see Fig. 13 and Fig. 14).

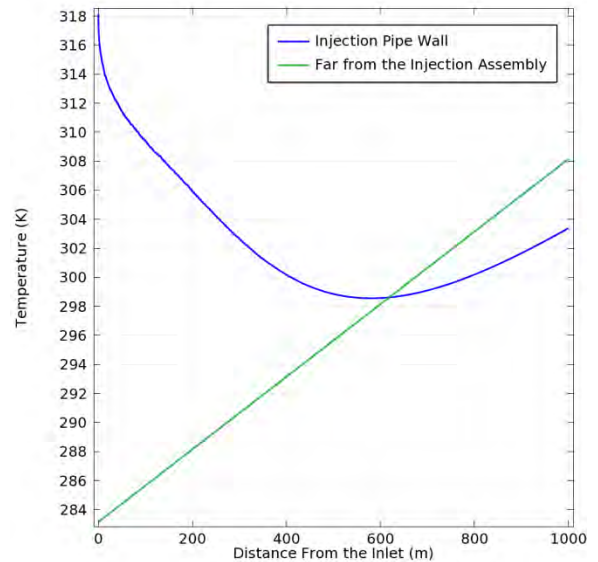


**Figure 13.** The temperature profile along the inner wall of the injection tubing and the temperature profile far from the injection assembly (inlet velocity = 0.01m/s)

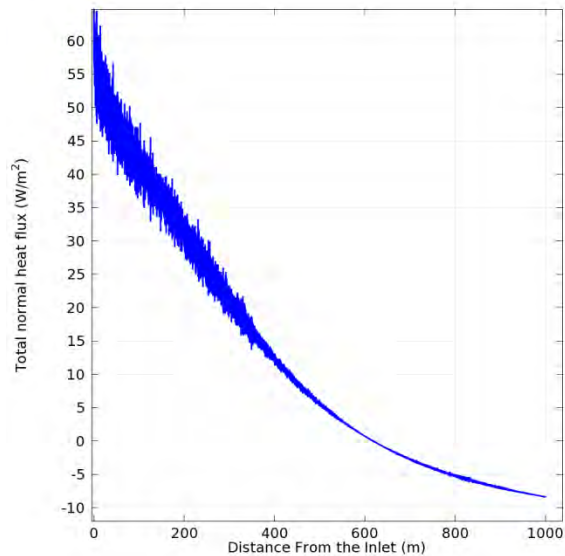


**Figure 14.** The heat flux at the inner wall of the injection tubing (inlet velocity = 0.01m/s)

## 6. Conclusions

In this work a model was created to simulate the heat transfer associated with a carbon sequestration well. The injection of supercritical carbon dioxide down a one kilometer injection well was simulated using COMSOL Multiphysics 4.2. The goal of the model was to investigate the thermal gradient present around the well and to determine the inversion point in the temperature and heat flux of the supercritical carbon dioxide.

Two simulations were done with an injection velocity of 0.001 and 0.1 m/s. An inversion point was observed in each of the simulations. Results indicate that as the injection velocity is increased the inversion point will be located deeper down the well. With an injection velocity closer to that of an actual carbon sequestration project (26 kg/s) this point may be much lower than the currently simulated 1 km. However, at higher velocities the heat transfer rates will be much higher as it will be a turbulent flow. Future simulation will center on simulating higher velocity turbulent flows and also integrating stratification of the formation.

## 7. References

1. Donald T. Secor, Jr., The role of Fluid Pressure in Jointing, *American Journal of Science*, **263**, 633-646 (1965)
2. Marie-Christine Duluc, Shihe Xin, Patrick Le Quere, Transient natural convection and conjugate transients around a line heat source, *International*

*Journal of Heat and Mass Transfer*, **46**, 341–354 (2003)

3. H.J. Ramey Jr., Mobil Oil Co., Wellbore Heat Transmission, *Journal of Petroleum Technology*, **14**, 427-435 (1962)

4. G.P. Willhite, Overall Heat Transfer Coefficient in Steam Injection well, *Journal of Petroleum Technology*, **19**, 607-616 (1967)

5. E.W. Lemmon, M.O. McLinden and D.G. Friend, Thermophysical Properties of Fluid Systems, in *NIST Chemistry WebBook, NIST Standard Reference Database Number 69*, Eds. P.J. Linstrom and W.G. Mallard, National Institute of Standards and Technology, Gaithersburg MD, <http://webbook.nist.gov>, (retrieved July, 2011).

## 8. Acknowledgment

The authors are grateful to the National Science and Engineering Research Council of Canada (NSERC) and the Canadian Foundation for Innovation (CFI).